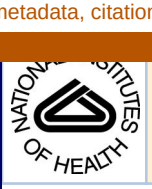

Published in final edited form as:

J Pharm Sci. 2015 February ; 104(2): 602–611. doi:10.1002/jps.24259.

DO NOT DROP: MECHANICAL SHOCK IN VIALS CAUSES CAVITATION, PROTEIN AGGREGATION AND PARTICLE FORMATION

Theodore W. Randolph[1], **Elise Schiltz**[1], **Donn Sederstrom**[2], **Daniel Steinmann**[3], **Olivier Mozziconacci**[3], **Christian Schöneich**[3], **Erwin Freund**[4], **Margaret S. Ricci**[4], **John F. Carpenter**[5], and **Corrine S. Lengsfeld**[2]

[1]Department of Chemical and Biological Engineering, University of Colorado Boulder, Boulder, CO

[2]Department of Mechanical and Materials Engineering, University of Denver, Denver, CO

[3]Department of Pharmaceutical Chemistry, University of Kansas, Lawrence, KS

[4]Process Development, Amgen, Inc., Thousand Oaks, CA

[5]Department of Pharmaceutical Sciences, University of Colorado Denver, Aurora, CO

Abstract

Industry experience suggests that g-forces sustained when vials containing protein formulations are accidentally dropped can cause aggregation and particle formation. To study this phenomenon, a shock tower was used to apply controlled g-forces to glass vials containing formulations of two monoclonal antibodies and recombinant human growth hormone (rhGH). High-speed video analysis showed cavitation bubbles forming within 30 μs and subsequently collapsing in the formulations. As a result of echoing shock waves, bubbles collapsed and reappeared periodically over a millisecond timecourse. Fluid mechanics simulations showed low-pressure regions within the fluid where cavitation would be favored. A hydroxyphenylfluorescein assay determined that cavitation produced hydroxyl radicals. When mechanical shock was applied to vials containing protein formulations, gelatinous particles appeared on the vial walls. Size exclusion chromatographic analysis of the formulations after shock did not detect changes in monomer or soluble aggregate concentrations. However, subvisible particle counts determined by microflow image analysis increased. The mass of protein attached to the vial walls increased with increasing drop height. Both protein in bulk solution and protein that became attached to the vial walls after shock were analyzed by mass spectrometry. rhGH recovered from the vial walls in some samples revealed oxidation of Met and/or Trp residues.

SUPPLEMENTAL MATERIAL

This article contains supplementary material available from the authors upon request or via the Internet at http://onlinelibrary.wiley.com/.

INTRODUCTION

To ensure drug product quality, it is important to retain the chemical and conformational purity of proteins during storage, shipping and delivery to patients. Of the many chemical degradation paths and physical instabilities to which proteins may be subjected, aggregation is one of the most prevalent[1]. The presence of aggregated proteins in certain cases has been associated with reduced efficacy, induction of unwanted immune responses, and anaphylactic shock[2,3].

One largely unrecognized cause of protein damage is mechanical shock to the primary drug product container. Vials and syringes that are dropped by patients or caregivers may experience severe mechanical shock, but unless the container shatters, the contents are typically administered without further examination. When dropped primary containers hit a solid surface, the solutions inside experience mechanical shock, and the resulting shock waves and associated fluid mechanics may cause cavitation. Cavitation is the formation, growth, and collapse of cavities in a liquid[4–6]. Cavities formed by mechanical forces imposed by the high g-forces that arise from the mechanical shock of dropping are unstable, and rapidly implode. When the cavities violently collapse, hot spots are created[4–8]. These extremely short-lived and localized hot spots are local regions of extremely high temperatures and pressure that may reach thousands of Kelvin and hundreds of atmospheres, respectively[4–8]. During the collapse of a cavity, hydrogen and hydroxyl radicals can also be formed[4,9–11].

As a result of the high temperatures, high pressures and free radical formation that occur during cavitation, protein molecules can be damaged[10]. For example, cavitation resulting from therapeutic ultrasound has been shown to cause structural changes in several different proteins including cytochrome c, lysozyme, bovine serum albumin, trypsinogen, RNAse and α-chymotrypsinogen[12, 1314]. Furthermore, hydroxyl radicals produced during cavitation have been shown to crosslink proteins and cause formation of protein particles[15,16].

There have been observations of shipping- and handling-induced aggregation and particle formation in formulations therapeutic proteins contained in their final drug product vials and prefilled syringes[17,18]. Furthermore, we hypothesize that if a patient or caregiver were to drop a vial onto a hard surface, undetected cavitation could occur, fostering formation of protein aggregates and proteinaceous particles. To simulate shock that could occur as a result of shipping and/or accidental dropping, a mechanical drop tester was used to apply controlled mechanical shock to glass vials containing formulations of two different monoclonal antibodies or recombinant human growth hormone. High speed video photography was used to record the formation and collapse of cavitation bubbles and fluid flows over sub-millisecond timescales. The formation of free radicals that formed during cavitation was confirmed by fluorescence spectroscopy using a hydroxyphenylfluorescein assay. Damage to the proteins was quantified by measuring aggregate levels with size exclusion chromatography, and subvisible particle counts made by microflow imaging. The protein adhering to the vial walls following shock treatment was also quantified. Chemical degradation of the proteins was assessed by high performance liquid chromatography and mass spectrometry.

MATERIALS AND METHODS

Model Proteins

Two model proteins were used for the majority of the studies: antistreptavidin IgG1 (provided by Amgen, Inc.) and recombinant human growth hormone (rhGH). Antistreptavidin was formulated at either 1 mg/mL or 35 mg/mL in 20 mM histidine buffer, pH 6. Recombinant human growth hormone (rhGH) was purified from inclusion bodies produced in E. coli[19] and formulated at 1.75 mg/mL in 2 mM sodium phosphate, pH 7.4. In a limited study to confirm video results, formulations containing a second monoclonal antibody (mAb1) at a concentration of 1 mg/mL in a 20mM histidine buffer, pH 6 were also examined.

Sample Preparation and Mechanical Shock Treatment

Protein formulations were filtered with a 0.2 um syringe filter prior to shock treatment. 4 mL sterilized borosilicate glass vials (West Pharmaceuticals, Lionville, PA) were rinsed with filtered water, filled with 1 or 4 mL of protein formulation and sealed at ambient pressure with chlorobutyl stoppers (West Pharmaceuticals, Lionville, PA) that had been rinsed with filtered water. To simulate the high g-forces and mechanical shock that may be sustained when a drug vial is dropped, a Lansmont Model 15D shock test system (Monterey, CA) was used. Vials were mounted using a custom-designed holder in an upright position on the falling block of the shock test system, and supported by a Teflon® base. Sample vials were dropped from heights ranging from 10 to 40 inches. Un-dropped samples (referred to as “0 in”) in identical vials were used as controls.

High Speed Video Analysis

In initial experiments, a Keyence (Osaka, Japan) VW-9000 high speed microscope was used to record images at a rate of 6000 frames per second of the vials as they underwent mechanical shock. In additional studies, a Phantom high-speed camera was used to record images at a rate of 66,666 frames per second during mechanical shock as vials containing either 1 or 3 mL of mAb1 formulation were dropped in the Lansmont shock test system.

Using the Phantom high speed camera, high speed images also were recorded of vials that were dropped by hand and contacted a hard surface after a free-fall of approximately 1 m. These vials struck the surface at various angles.

Hydroxyphenyl Fluorescein Assay to Detect Cavitation-Induced Free Radicals

In the presence of free radicals, hydroxyphenyl fluorescein forms the highly fluorescent product fluorescein. Hydroxyphenyl fluorescein (Invitrogen, Carlsbad, CA) was added to the 1 mg/mL protein solutions to a concentration of 5 μM, and 1mL of the resulting solution filled into 4 mL vials. Following shock treatment, the samples were placed in a fluorometer (SLM 8000, SLM, Urbana, IL) After excitation at 490 nm, fluorescence emission intensity of the samples was measured at 515 nm. A fluorescein standard curve was used to determine the concentration of fluorescein in the samples.

Size Exclusion Chromatographic Analysis of Soluble Aggregates and Monomeric Protein

Samples were analyzed using size exclusion chromatography to determine the amount of monomeric protein and soluble aggregates before and after mechanical shock treatment. Prior to analysis, samples were centrifuged for 10 minutes at 9,300g to pellet any insoluble material. Size exclusion chromatography was carried out using a Beckman HPLC system (Beckman Coulter Inc, Fullerton, CA). For analysis of antistreptavidin samples, the mobile phase was 100 mM sodium phosphate, 300 mM sodium chloride, 0.01% sodium azide, pH 7, and a flowrate of 0.6 mL/min was used. For analysis of rhGH samples, the mobile phase consisted of 25 mM ammonium bicarbonate, 0.01% sodium azide, pH 7.4, and 1 mL/min flowrate was used. For both of the proteins, 100 μL injections on a TSK-GEL G3000SWXL column with an SW guard column were used. Absorbance at 280 nm was measured.

Microflow Imaging Analysis of Sub-visible Particulates

A benchtop FlowCAM (Fluid Imaging Technologies, Yarmouth, ME) was used to image and count particles of sizes greater than or equal to 2 μm. A 10x objective and 100 μM flowcell were used to analyze 215 μL of sample per assay. Between samples, the flowcell was flushed with water that had been filtered through a 0.2 μm filter.

Recovery and Quantification of Protein Adhered to Vial Wall after Cavitation

Two methods were used to recover protein that had adhered to vial walls. The first method used urea to dissolve protein from the vial walls. Following shock treatment, all liquid was removed from the vials with a pipette. The vials were rinsed twice with 1 mL formulation buffer to remove un-adhered protein, and 250 μL of 8 M urea was added to the vials. The samples were then incubated overnight at room temperature with mixing on a rotator such that the urea solution contacted the entire vial wall surface. The next day, the urea solution was diluted 4x in order to be compatible with a standard Bradford total protein assay. Bradford reagent and the diluted urea solutions were mixed in a 1:1 ratio, incubated at room temperature for 5 minutes, and the absorbance at 595 nm was measured and compared to that for a placebo blank. A standard curve using the same protein and buffer as that in the mechanically-shocked samples was used.

A second method used guanidine hydrochloride solution to remove the protein from the vial walls. Following mechanical shock treatment, the solution was removed from the vials with a pipette. Residual solution was then removed by rinsing the vials twice with 1 mLbuffer. Finally, 0.5 mL of 7.5 M guanidine hydrochloride, 0.25 M tris, pH 7.5 was added to the vials and incubated overnight at room temperature mixing on a rotator such that guanidine could access all of the vial wall surface. The next day, the absorbance was measured at 280 nm to determine the amount of protein recovered from the vial walls. Absorbance values were corrected by subtracting absorbance values for appropriate buffer blanks.

Tryptic Digestion/HPLC Analysis of Protein Degradation

Samples from the bulk solution and samples recovered from the washed vial walls were enzymatically digested following shock treatment using trypsin. For antistreptavidin samples, a protocol similar to that developed by Ren, et al.[20] was used. All of the bulk solution was removed from the vials after shock treatment. The bulk solution was diluted

into denaturation buffer (7.5 M guanidine hydrochloride, 0.25 M tris, pH 7.5) to a final concentration of 1 mg/mL and a final volume of 500 μL. After the solution was removed from the vials, they were rinsed with buffer. 500 μL of denaturation buffer was added to the vials and incubated overnight to recover protein from the vial walls. The next day, 3 μL of 0.5 M DTT were added to all samples and incubated at room temperature for 30 minutes. Next, 7 μL of 0.5 M iodoacetic acid was added and incubated in the dark for 15 minutes. 4 μL of 0.5 M DTT were added to the samples and samples were buffer exchanged into digestion buffer (0.1 M tris, pH 7.5) using NAP-5 columns (GE Healthcare, Piscataway, NJ). Trypsin was added to the samples in a 1:25 trypsin:antistreptavidin ratio and incubated at 37 °C for 30 minutes. The reaction was quenched with 5 μL of 20% formic acid. Reversed phase chromatography analysis was conducted using a Phenomenex (Torrance, CA) Jupiter C18 column on an Agilent (Palo Alto, CA) 1100 Series system. The flowrate was 0.2 mL/min and a linear gradient of 0–50% B (Buffer A: 0.1% trifluoroacetic acid, Buffer B: 90% acetonitrile, 0.085% trifluoroacetic acid) over 195 minutes was used for elution. Absorbance at 215 nm was measured.

For rhGH samples, following shock treatment, all bulk solution was removed from vials, and the vials were rinsed with buffer. Bulk solution and the vials were frozen separately at −80°C and shipped on dry ice to The University of Kansas, where trypsin or chymotrypsin digestion and mass spectroscopy analysis were performed on the samples. Samples of the bulk solutions that had not been subjected to shock treatment were used as controls. For the bulk solution samples, 10 μL of sample was digested with 50 μL of trypsin or chymotrypsin solution (20 μg/mL in 0.1 M ammonium bicarbonate, pH 7.8) at 37°C overnight. For analysis of protein adhering to vial walls, 50 μL of trypsin solution was added directly to the vials and the protein adhering to the vial walls was digested overnight at 37°C. Following digestion, LC-MS analysis was run with a Presto-FF-C18 column. A 1 hour gradient from 10–50% acetonitrile was used followed by a shorter gradient to 80% acetonitrile for washing. The chromatographic system used was an Acquity UPLC system (Waters Corp., Milford, MA) coupled to a SYNAPT-G2 (Waters Corp., Milford, MA) mass spectrometer. The flow rate was 20 μL/min. The SYNAPT-G2 instrument was operated for maximum resolution with all lenses optimized on the $[M+2H]^{2+}$ ion from the $[Glu]^1$-fibrinopeptide B. The cone voltage was 45 V and AR was admitted to the collision cell. The spectra were acquired using a mass range of 50–2000 amu. The data were accumulated for 0.7 sec per cycle. Data were analyzed with the ProteinLynx Global Server from Waters Corp. (Millford, MA). Specific oxidation yields were calculated through the integration of peak areas in the extracted ion chromatogram of the most abundant ion of the respective tryptic peptide. It was assumed that the electrospray-ionized peptides of any oxidative modifications have similar mass spectrometric properties as the respective ions of the native peptides due to the small mass difference.

Computational Fluid Dynamics Calculations of Mechanical Shock-Induced Cavitation

The transient behavior of fluid within a vial impacting a solid surface was modeled using Fluent's (ANSYS, Inc., Canonsburg, PA) Volume of Fluid (VOF), axisymmetric solver with the Reynolds Averaged Navier-Stokes (RANS) turbulence model described by the realizable k-ε closure model. A pressure-velocity coupled algorithm was used to calculate the flow

field with a 2nd order discretization for the momentum, turbulence, and energy equations. Vials were modeled as containing water in the bottom 1/3rd of the vial with air at 1 atm in the remaining area with appropriate meniscus height and shape. The wall boundaries were modeled with no-slip conditions using standard wall functions to account for the viscous boundary layer at the surface of the vial. The temperatures for all the boundary conditions were set to 293K. The fluid used in the comparison of simulated results to experimental data for model validation was water at standard temperature and pressure. The Ideal Gas Law was selected to allow compressible behavior of the gas phase and a user-defined function implemented for the compressible behavior of the liquid phase. The compressibility of water as a function of pressure was calculated using the bulk modulus of water. A sliding wall mesh was utilized to simulate the fall and rebound of the vial.). Initial fluid velocities matched the wall's downward velocity at impact Three impact cases were evaluated to simulate dropping a vial of containing water from a height of 90 cm onto "soft" and "hard" surfaces: (i) a soft, 5-cm foam-padded surface, yielding an impact of 50g, (ii) a soft, 1-cm foam-padded surface, yielding an impact of 500g, and (iii) a hard metal surface, with a corresponding impact of 5000g. These gravitation accelerations were estimated from high-speed images using the vial geometry, recorded vial positions and the video frame rate to determine velocities immediately before and after contact. The 90-cm drop heights was chosen to correspond drop distances that a vial might experience when falling off a counter or out of a user's hand.

A total of 21,219 quadrilateral elements were used to achieve a high quality computational mesh, resulting in an average mesh density of 2,072 per square millimeter. The maximum cell skewness was 0.50, and the minimum orthogonal quality of 0.79. The maximum growth rate from one element to the next was 10%. Convergence criteria for the computational domains were met when the residuals for pressure, momentum, and turbulence were below 10^{-3} and below 10^{-6} for the energy equation.

RESULTS

Indications of Cavitation

High Speed Video Analysis—To visualize fluid motion and cavitation occurring in liquids within partially-filled vials during shock treatment, high speed video of antistreptavidin formulations in partially-filled vials was captured as the vials were dropped in the Lansmont Model 15D shock test system. Figure 1 shows selected time lapse images of a representative vial during shock treatment; full video is available in the supplementary material. Time 0 represents the time point when the vial hit the bottom platform of the shock tower and began to rebound. As the vial began to rebound, the meniscus inverted, and a jet of liquid shot up towards the top of the vial. As the jet formed, cavitation bubbles could be seen near the bottom of the vial at about 500 μs after impact. The cavitation bubbles quickly collapsed within a few hundred microseconds.

Similar cavitation was also observed when mAb1 solutions in the same type of 4mL vials were dropped in the Lansmont Model 15D shock test system from a height of 40 inches (Figure 2). Cavitation was evident in images recorded after 165 μs. Vials filled with 3 mL of mAb1 solution showed more extensive cavitation than vials filled with 1 mL, and the

cavitation bubbles that were produced appeared to oscillate in size. After some of the bubbles collapsed, new cavitation events rapidly followed, suggesting that shock waves emanating from the collapsing primary cavitation sites and/or that echoes of the original shock wave caused additional bubble formation. Cavitation was not observed when vials were filled with deionized water (Figure 3).

When the orientation of the vial upon contact with a hard surface was varied by hand-dropping vials containing 1 mg/mL mAb1 solutions and allowing them to free-fall for ~1m, cavitation was observed. In these vials, the pattern and position of the cavitation bubbles were highly variable, depending on the orientation of the vials at the point of contact with the surface. Occasionally, vial breakage was observed as a result of the free-fall drops; no attempt was made to recover or analyze samples in vials that broke. A representative sequence of high-speed video images for a square impact between the vial and the surface is shown in Figure 4, and for an angled impact in Figure 5; full video sequences are provided in the supplementary material. In these studies, where images were recorded using the Phantom camera at very high speeds, cavitation could be observed within 30 μs after the falling vial contacted the hard surface.

Hydroxyphenyl Fluorescein Assay—Because collapse of cavitation bubbles was expected to produce free radicals, hydroxyphenyl fluorescein (HPF) was used to detect hydroxyl radicals produced during mechanical shock treatment. Upon reacting with a hydroxyl radical, HPF is converted to the fluorescent molecule fluorescein[21]. HPF was added to vials prior to mechanical shock treatment and the fluorescence intensity was measured after treatment. A fluorescein standard curve was used to determine the concentration of fluorescein produced during shock treatment, and the results are shown in Figure 6. Between 20 and 40 nM of fluorescein were detected in the vials after shock treatment. The quantity of fluorescein that is formed is only a qualitative indicator of the formation of free radicals, because the free radicals that are produced during cavitation would be expected to react not only with HPF but also with the buffer and protein. Thus, it is likely that far more than 20–40 nM of free radicals were formed as a result of shock treatment.

Results of Computational Fluid Dynamics Calculations—Numerical simulations of the fluid behavior, in particular pressure-field characteristics, were conducted under each of the three impact cases (described in the Methods) to assess whether the conditions for cavitation would be satisfied and in what regions of the vial such conditions might occur. Figure 7 shows the computed pressure fields within the vials. At the bottom of each of the vials is a low pressure region, with the magnitude of the low pressure being dependent on the drop conditions. Each of the three impact cases has the same maximum pressure in the upper portion of the vial, but the low pressure magnitudes are greatly different. The vapor pressure of the water in these simulations is 3.5 kPa. Vials dropped on “soft” surfaces, which produce shock that might be typical of that experienced by the contents of a vial that has been protected by secondary packaging, are higher than 3.5 kPa, whereas vials dropped on “hard” surface showed low pressures well below the vapor pressure of water. This indicates that only the hard-impact, metal on metal case is likely to cause cavitation.

Analysis of Bulk Liquid Within Mechanically-Shocked Vials

Following shock treatment, the solution from dropped and control non-dropped vials was removed and analyzed for protein aggregates, particles, and protein chemical damage.

Size Exclusion Chromatography—Size exclusion chromatography was used to measure the concentrations of monomer and soluble aggregates in the bulk solution following shock treatment. For all sample types tested (1.0 mg/mL antistreptavidin, 35 mg/mL antistreptavidin, and 1.75 mg/mL human growth hormone), no significant loss of monomer or increased level of soluble aggregates resulting from application of mechanical shock could be detected by size exclusion chromatography (data not shown).

Particle Count and Size Distribution—FlowCAM microflow imaging analysis was used to count and size particles of size equal to or greater than 2 μm in 1 mL samples of each of three formulations (antistreptavidin at 1 or 35 mg/mL, and rhGH at 1.75 mg/mL) following application of mechanical shock to vials (Figures 8a,c,e). Shock treatment resulted in an increase in the number of particles. Drop height did not appear to have a large effect on the number of particles counted; all drop heights produced about the same number of particles for a given protein and protein concentration. For both antistreptavidin and rhGH, a large fraction of the particles that formed after application of mechanical shock showed long, fibrillar aspect ratios (Figures 8b,d,f).

In a separate experiment to determine the effect of fill volume on particle formation, a set of samples was prepared by filling vials with either 1 or 4 mL of a 1.75 mg/mL rhGH formulation. These vials were dropped from a height of 40 inches in the Lansmont shock tester. In vials filled with 4 mL solution, cavitation was more apparent than in the vials with a 1 mL fill volume. The concentrations in the solution of microparticles of size equal to or greater than 2 μm were measured before and after shock treatment using the FlowCam instrument. Prior to shock testing, an average of 11,100 particles of size equal to or greater than 2 μm/mL were detected in the rhGH solutions. After a single drop, the particle concentrations increased to 16,800±700 particles/mL in vials filled with 1mL of solution, and to 31,300±3,500 particles/mL in vials filled with 4 mL of solution.

Tryptic Digestion/RP-HPLC Analysis of Protein Degradation—Trypsin digestion followed by reverse-phase HPLC was used to monitor chemical damage to the protein as a result of shock treatment. The bulk solution from 35 mg/mL antistreptavidin samples was digested with trypsin and analyzed on reversed phase chromatography. No chemical differences in proteins remaining in the bulk solution were detected in the dropped samples compared to the control samples (data not shown).

Bulk solution rhGH samples were also digested with trypsin and analyzed by mass spectroscopy. Both control samples and samples of bulk solution dropped from a height of 40 inches showed similar levels of oxidation of methionine-14, methionine-125, methionine-170, and tryptophan (about 1% oxidation or less, data not shown).

Analysis of Protein Recovered from Vial Walls

Following shock treatment, gelatinous specks of protein were easily visible on the vial walls. The protein that adhered to the vials walls in the form of these gelatinous globules was recovered and quantified and analyzed for chemical damage.

Quantification of Recovered Protein—The protein adhering to the vial walls was recovered using guanidine or urea to remove the protein from the vial walls and quantified using the absorbance at 280 nm and the Bradford assay, respectively. The amount of protein recovered per vial is shown in Figure 9. In all cases, guanidine was more effective at removing adherent protein from the vial walls than was urea. Although the efficiency with which protein could be recovered from the vial walls was different depending on whether guanidine or urea were used, in both cases (and for both proteins tested) the amount of protein that adhered to the walls and could be removed for analysis increased as the drop height was increased in the mechanical shock tester.

Trypsin Digestion—After recovering the protein with guanidine, trypsin or chymotrypsin digestion and reverse-phase chromatography was used to monitor any chemical modifications to the protein. Chemical damage as a result of shock treatment was not detected for the 35 mg/mL antistreptavidin samples (data not shown).

Following recovery from the vial walls, rhGH samples were digested and analyzed by mass spectroscopy with focus on the oxidation of Met and Trp. Five series of samples were analyzed after trypsin digestion, where large sample-to-sample variations were recorded. For example, series 1 clearly indicated a significant increase of oxidation of Met-14 to Met sulfoxide (MetSO) and the single Trp residue compared to controls, while series 2 showed only a significant increase of oxidation of Met-170. Series 3 and 4 failed to indicate any significant increase of oxidation compared to controls, while series 5 showed an increase in Met-14 oxidation only for vials containing 4 mL solution and dropped from 40 inches height. Series 5 was also analyzed after chymotrypsin digestion of rhGH, which did not show significant oxidation of Met-14 to MetSO. It is possible, that digestion by one enzyme vs. another enzyme can bias towards certain products. However, at this point we can only conclude that oxidation of Met and Trp *may* be possible, but cannot be consistently observed. This result is consistent with the large sample-to-sample variations in cavitation observed by the high speed camera. In this context it is also important to note that hydroxyl radicals, generated via cavitation, react rather unselectively with proteins targeting all 20 amino acids, though with different rate constants[22]. Upon reaction with Met, hydroxyl radicals initially generate sulfide radical cations, which subsequently decompose into α-(alkylthio)alkyl radicals, whereas MetSO is not a primary product of Met oxidation by hydroxyl radicals unless superoxide is generated simultaneously[23] It appears that, wherever observed, MetSO formation in rhGH may be a consequence of secondary processes, i.e. peroxyl radical or peroxide formation.

DISCUSSION

Inadvertent dropping of vials and syringes almost certainly occurs in the clinic and during in–home administration of therapeutic protein formulations. Clearly, such events have the

potential to cause cavitation, since in the present study, even the relatively minor shock incurred when vials dropped only 10 inches onto hard surfaces caused cavitation. In turn, the violent collapse of cavitation bubbles and the resulting free radicals, high temperatures, and secondary shock waves may be likely to cause localized oxidative and conformational damage to proteins.

In the numerical simulations, of the calculated pressure fields within fluids subjected to a high acceleration collision (such as that typical of a dropped vial) indicate the generation of high-pressure shock waves and associated low-pressure, cavitation-prone regions along the bottom surface of the vial. The strength, location and timing of this low pressure region are consistent with the high-speed imaging of large vapor bubble formation within a vial under similar conditions. The application of energy-absorbing materials such as those that might be used in secondary packaging can mitigate this issue, as clearly demonstrated by the two soft-impact conditions. Under these conditions, neither a shock wave discontinuity in the pressure field nor a pressure region with pressures below the vapor pressure of water is observed. Future numerical studies are focusing on understanding the exact roles that dynamics (acceleration), vial shape and fluid properties (density, surface tension, viscosity, etc.) play in establishing the shock wave and dictating the magnitude of the low-pressure region.

In the bulk solution of the vials, there were no detectable changes in monomer or soluble aggregate concentrations after the vial contents were subjected to mechanical shock. This is not surprising, since the energy released upon collapse of a cavitation bubble is expected to be concentrated in an extremely small volume. There were also no visible insoluble aggregates formed in the bulk solution following mechanical shock treatment; all of the visible aggregates appeared to be attached to the vial walls. However, there was an increase in the number of subvisible particles of size greater than or equal to 2 μm detected by microflow imaging analysis following shock treatment. The ability of microflow imaging techniques to detect protein aggregates at levels below the sensitivity limit for size exclusion chromatographic analysis has been documented[24]. Mechanical shock treatment of samples formulated at the higher concentration of antistreptavidin generated more particles than did shock treatment of samples formulated at the lower concentration of antistreptavidin (Figure 8). Again, this might be expected if only protein in a small volume surrounding a collapsing cavitation bubble is damaged. Over the range of drop heights tested, the increase in subvisible particles in samples subjected to mechanical shock compared to un-dropped samples was not dependent on drop height, perhaps suggesting a threshold value of mechanical shock is required to create cavitation associated formation of particles.

Joubert, et al., characterized the aggregates of antibodies exposed to various types of stress[25]. Based on size and morphology, the aggregates produced as a result of shock treatment most closely resemble the aggregates produced during mechanical stresses such as agitation and stirring in their classification scheme. This might indicate that, in addition to the effects of cavitation-induced free radicals, the mechanical stresses caused by cavitation could also play an important role in generating protein aggregates.

After shock treatment, protein aggregates adhering to the vial walls were visible. The amount of protein recovered from the vial walls increased as drop height increases and was concentration dependent. More protein was recovered from the vial walls following shock treatment of 35 mg/mL antistreptavidin than was recovered following shock treatment of 1 mg/mL antistreptavidin. The amount of adherent protein scaled roughly with protein concentration. The protein that adhered to the wall of the vial after application of mechanical shock was difficult to remove, and resisted rinsing by buffer solutions. We speculate that the adherent properties of the gelatinous globules on the walls may have resulted from the potential oxidative damage and subsequent chemical crosslinking that resulted from the free radicals and high temperatures produced as cavitation bubbles collapsed, or from mechanical stresses caused by shock waves associated with collapse of cavitation bubbles.

In vials filled with deionized water with no added protein or buffer, we did not see video evidence of cavitation caused by the mechanical shocks that we applied. In previous work, we have shown that DNA molecules may serve as nucleation sites for cavitation[26]. We speculate that in the present case, protein molecules may play a similar role. Likewise, surfactant micelles, although not examined in this study, might also be able to serve as nucleation sites for cavitation.

In all of our studies, the cavitation phenomenon was highly variable from sample to sample. High speed video images showed that the number and location of cavitation sites were different in every sample tested, perhaps as a result of subtle differences in shape of the interior bottom surface of each vial. The sample-to-sample variation was even more apparent in the samples that were hand-dropped and thus contacted the surface at a various random angles.

The levels and types of chemical damage that were observed in the proteins were also quite variable. This variation was consistent not only with the variable cavitation levels that were observed by high-speed photography, but also with the inherent difficulties in sampling the damaged protein, which had formed small, adherent, gelatinous particles on the vial walls that were difficult to rinse off with buffer, instead requiring urea or guanidine HCL to remove them.

Chemical changes to antistreptavidin adhering to the vial walls were not detected, but in many rhGH samples where cavitation had occurred extensive oxidation was also observed. We hypothesize this damage to rhGH is due to the reactive oxygen species such as OH radicals produced during cavitation reacting with the protein. A possible explanation for the lack of oxidative damage detected in the antistreptavidin sample might be the lack of sensitivity of our analytical technique to potential oxidative damage in the relatively large mAb molecule, wherein oxidative damage might have been dispersed over a larger number of residues. In addition, because our peptide-focused mass spectrometry technique is not sensitive to glycan chemical changes, damage would not be detected if the OH radicals reacted preferentially with the highly solvent-exposed glycosylated portion of the molecules.

CONCLUSIONS

The mechanical shock caused by dropping unprotected (e.g., not packaged in protective secondary packaging) glass vials containing liquid formulations of therapeutic protein from heights as low as 10 inches was sufficient to cause cavitation in the liquid, as evidenced high speed video and the production of hydroxyl radicals detected by hydroxyphenyl fluorescein. Numerical simulations were consistent with high speed video and showed that cavitation may be mitigated by energy absorbing materials, such as those often found in secondary packaging.

As a result of this cavitation, subvisible particles were created in the bulk solution of the vials. In addition, protein particles were visible on the vial walls following shock treatment. The amount of protein adhering to the vial walls increased with drop height. For rhGH, the protein adhering to the vial walls following shock treatment showed increased levels of oxidation.

The loss of monomeric protein due to cavitation likely was not large enough to affect potency of protein in the bulk solution. However, the mechanical shock caused subvisible particles to form, and such particles have the potential to affect immunogenicity of the formulation[27]. Thus, packaging, formulation excipient composition, and process conditions should be designed to minimize mechanical shock and the potential for cavitation.

Supplementary Material

Refer to Web version on PubMed Central for supplementary material.

Acknowledgments

Funding for this work was provided by Amgen, Inc. and through the NIH #5RO1 EB006006.

References

1. Wang W, Singh S, Zeng D, King K, Nema S. Antibody structure, instability, and formulation. Journal of Pharmaceutical Sciences. 2007; 96(1):1–26. [PubMed: 16998873]
2. Rosenberg AS. Effects of Protein Aggregates: An Immunological Perspective. AAPS Journal. 2006; 8(3):E501–E507. [PubMed: 17025268]
3. Kessler M, Goldsmith D, Schellekens H. Immunogenicity of biopharmaceuticals. Nephrology Dialysis Transplantation. 2006; 21:9–12.
4. Thompson L, Doraiswamy L. Sonochemistry: Science and engineering. Industrial & Engineering Chemistry Research. 1999; 38(4):1215–1249.
5. Suslick KS, Flannigan DJ. Inside a collapsing bubble: Sonoluminescence and the conditions during cavitation. Annual Review of Physical Chemistry. 2008; 59:659–683.
6. McNamara W, Didenko Y, Suslick K. Sonoluminescence temperatures during multi-bubble cavitation. Nature. 1999; 401(6755):772–775.
7. Flannigan D, Suslick K. Plasma formation and temperature measurement during single-bubble cavitation. Nature. 2005; 434(7029):52–55. [PubMed: 15744295]
8. Didenko Y, McNamara W, Suslick K. Temperature of multibubble sonoluminescence in water. Journal of Physical Chemistry a. 1999; 103(50):10783–10788.

9. PESTMAN J, ENGBERTS J, DEJONG F. SONOCHEMISTRY - THEORY AND APPLICATIONS. Recueil Des Travaux Chimiques Des Pays-Bas-Journal of the Royal Netherlands Chemical Society. 1994; 113(12):533–542.

10. RIESZ P, KONDO T. FREE-RADICAL FORMATION INDUCED BY ULTRASOUND AND ITS BIOLOGICAL IMPLICATIONS. Free Radical Biology and Medicine. 1992; 13(3):247–270. [PubMed: 1324205]

11. RIESZ P, BERDAHL D, CHRISTMAN C. FREE-RADICAL GENERATION BY ULTRASOUND IN AQUEOUS AND NONAQUEOUS SOLUTIONS. Environmental Health Perspectives. 1985; 64:233–252. [PubMed: 3007091]

12. Marchioni C, Riccardi E, Spinelli S, Dell'Unto F, Grimaldi P, Bedini A, Giliberti C, Giuliani L, Palomba R, Castellano A. Structural changes induced in proteins by therapeutic ultrasounds. Ultrasonics. 2009; 49(6–7):569–576. [PubMed: 19278707]

13. EDWARDS J, JAMES C, COAKLEY W, BROWN R. EFFECT OF ULTRASONIC CAVITATION ON PROTEIN ANTIGENICITY. Journal of the Acoustical Society of America. 1976; 59(6):1513–1514. [PubMed: 939885]

14. Gulseren I, Guzey D, Bruce B, Weiss J. Structural and functional changes in ultrasonicated bovine serum albumin solutions. Ultrasonics Sonochemistry. 2007; 14(2):173–183. [PubMed: 16959528]

15. SUSLICK K, GRINSTAFF M, KOLBECK K, WONG M. CHARACTERIZATION OF SONOCHEMICALLY PREPARED PROTEINACEOUS MICROSPHERES. Ultrasonics Sonochemistry. 1994; 1(1):S65–S68.

16. GRINSTAFF M, SUSLICK K. AIR-FILLED PROTEINACEOUS MICROBUBBLES - SYNTHESIS OF AN ECHO-CONTRAST AGENT. Proceedings of the National Academy of Sciences of the United States of America. 1991; 88(17):7708–7710. [PubMed: 1652761]

17. Ricci, M.; Donahue, L.; Ball, N.; Stackhouse, N.; Lee, J.; Krishnan, S.; Pallitto, M. Silicone oil induced particle formation in prefilled syringes. 236th ACS National Meeting; August 17–21; Philadelphia, PA: American Chemical Society; 2008.

18. Bonk, REB.; Huinker, A.; Pallitto, M.; Ricci, M.; Stackhouse, S. Stabilized protein compositions. Patent WO2009099641A2. 2009. Stabilized protein compositions. ed

19. Fradkin AH, Boand CS, Eisenberg SP, Rosendahl MS, Randolph TW. Recombinant Murine Growth Hormone from E. coli Inclusion Bodies: Expression, High-Pressure Solubilization and Refolding, and Characterization of Activity and Structure. BIOTECHNOLOGY PROGRESS. 2010; 26(3):743–749. [PubMed: 20196161]

20. Ren D, Pipes G, Liu D, Shih L, Nichols A, Treuheit M, Brems D, Bondarenko P. An improved trypsin digestion method minimizes digestion-induced modifications on proteins. Analytical Biochemistry. 2009; 392(1):12–21. [PubMed: 19457431]

21. Setsukinai K, Urano Y, Kakinuma K, Majima H, Nagano T. Development of novel fluorescence probes that can reliably detect reactive oxygen species and distinguish specific species. Journal of Biological Chemistry. 2003; 278(5):3170–3175. [PubMed: 12419811]

22. Davies M. The oxidative environment and protein damage. Biochimica Et Biophysica Acta-Proteins and Proteomics. 2005; 1703(2):93–109.

23. Schöneich C. Methionine oxidation by reactive oxygen species: reaction mechanisms and relevance to Alzheimer's disease. Biochim Biophys Acta. 2005; 1703(2):111–119. [PubMed: 15680219]

24. Barnard JG, Singh S, Randolph TW, Carpenter JF. Subvisible particle counting provides a sensitive method of detecting and quantifying aggregation of monoclonal antibody caused by freeze-thawing: Insights into the roles of particles in the protein aggregation pathway. J Pharm Sci. 2010

25. Joubert MK, Luo QZ, Nashed-Samuel Y, Wypych J, Narhi LO. Classification and Characterization of Therapeutic Antibody Aggregates. Journal of Biological Chemistry. 2011; 286(28):25118–25133. [PubMed: 21454532]

26. Lentz YK, Anchordoquy TJ, Lengsfeld CS. DNA acts as a nucleation site for transient cavitation in the ultrasonic nebulizer. Journal of Pharmaceutical Sciences. 2006; 95(3):607–619. [PubMed: 16432878]

27. Rombach-Riegraf V, Karle AC, Wolf B, Sordé L, Koepke S, Gottlieb S, Krieg J, Djidja MC, Baban A, Spindeldreher S, Koulov AV, Kiessling A. Aggregation of human recombinant monoclonal antibodies influences the capacity of dendritic cells to stimulate adaptive T-cell responses in vitro. PLoS One. 2014; 9(1):e86322. [PubMed: 24466023]

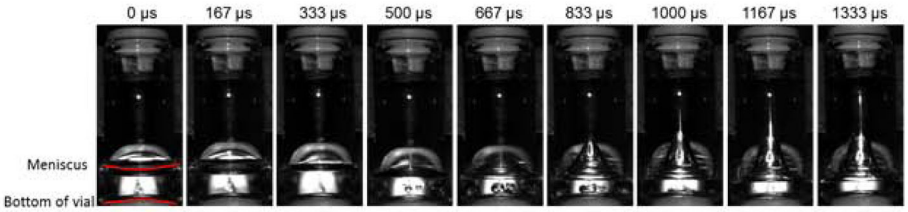

Figure 1.

Time lapse images of fluid in a partially filled vial as it contacts a solid surface after being dropped from a height of 40 inches. In the third frame, recorded 500 microseconds after contact, two large cavitation bubbles become visible. These cavitation bubbles collapse rapidly, with complete collapse occurring around 1000 microseconds after the initial contact.

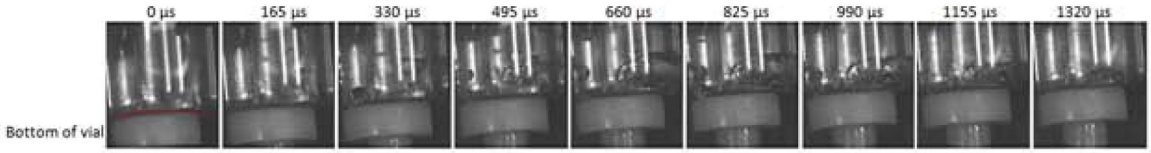

Figure 2.

Time lapse images of mAb1 solution in a fully filled vial as it contacts a solid surface after being dropped from a height of 40 inches. In the third frame, recorded 330 microseconds after contact, many large bubbles appear and grow until they begin to collapse in the seventh frame labeled 990 microseconds. These cavitation bubbles collapse rapidly, with complete collapse occurring around 1300 microseconds after the initial contact. The Teflon® bumper on which the vials were mounted in the mechanical shock tester is visible in the bottom of each frame.

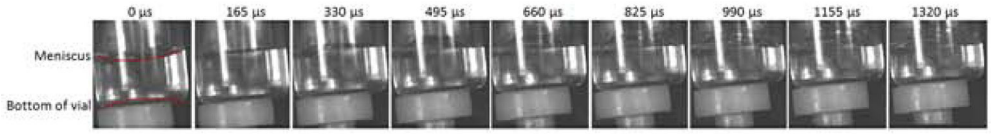

Figure 3.

Time lapse images of deionized water in a partially filled vial as it contacts a solid surface after being dropped from a height of 40 inches. There is no evidence for any bubble formation or cavitation in any of the images,

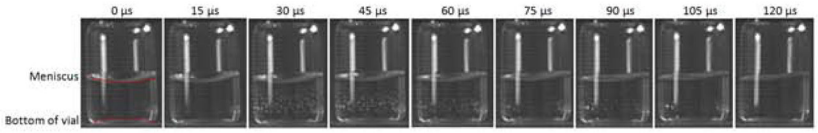

Figure 4.

Time lapse images of a 1 mg/ml mAb formulation in a partially filled vial as it contacts a solid surface squarely after being dropped from a height of 1 m without the aid of a shock tower. In the third frame, recorded 30 microseconds after contact, many small bubbles rapidly appear and disappear in an oscillatory fashion until they completely disappear in the ninth frame labeled 120 microseconds.

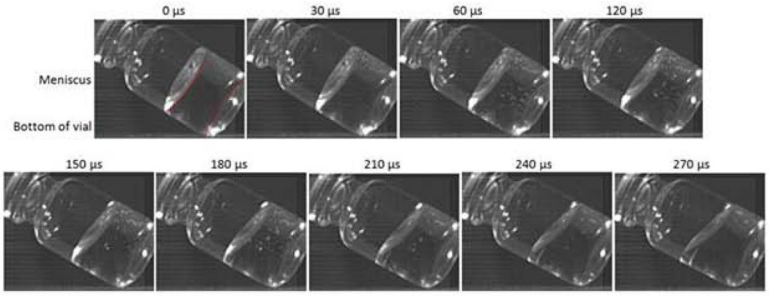

Figure 5.

Time lapse images of fluid in a partially filled vial containing 1 mg/ml mAb as it contacts a solid surface at an angle after being dropped from a height of 1 m without the aid of a shock tower. In the second frame, recorded 30 microseconds after contact, many small bubbles appear and rapidly disappear, until they almost completely disappear in the ninth frame labeled 270 microseconds.

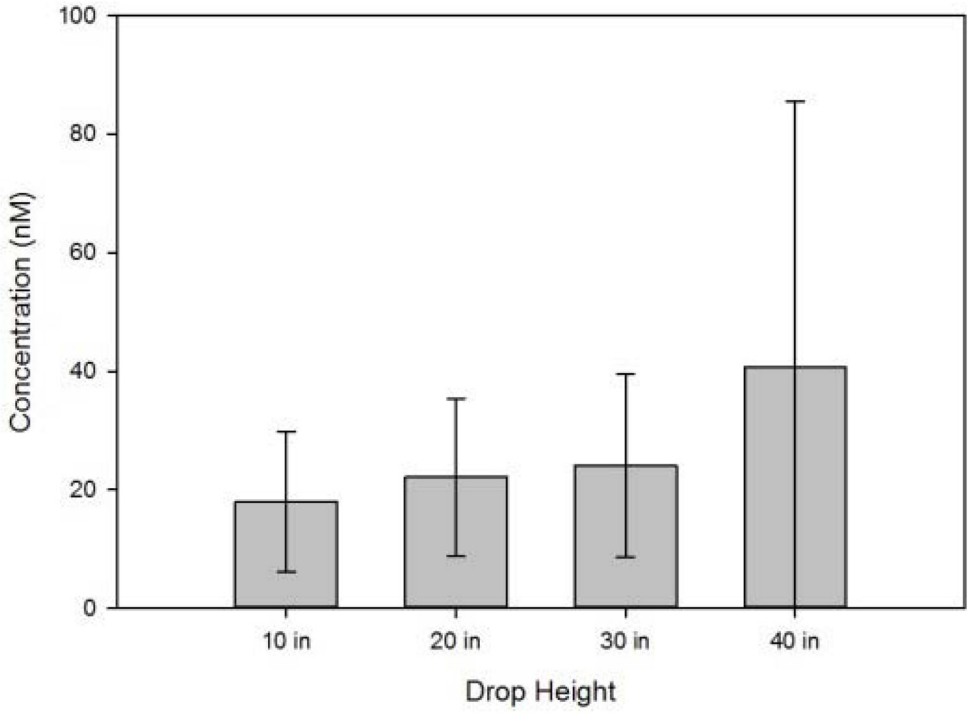

Figure 6.

Concentration of fluorescein liberated from reaction of p-phenylfluorescein with hydroxyl radicals generated during shock treatment as a function of drop height. Concentrations were determined from the difference in fluorescence between fluid in mechanically-shocked vials and fluid in identical, untreated control vials.

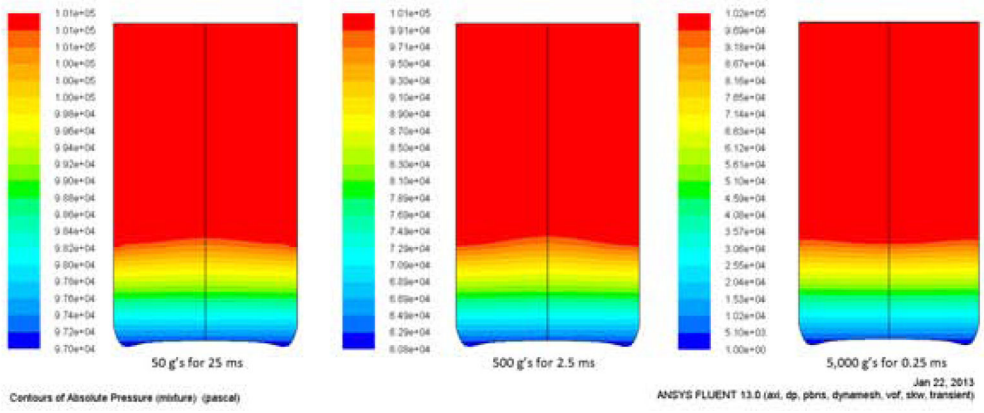

Figure 7.

Numerical simulation of 1/3rd filled vial with water being dropped from 90 cm impacting under the following conditions: (left) a 2.0″ foam padded impact (50g), (center) a 0.5″ foam padded impact (500g), and (right) a metal surface (5000g).

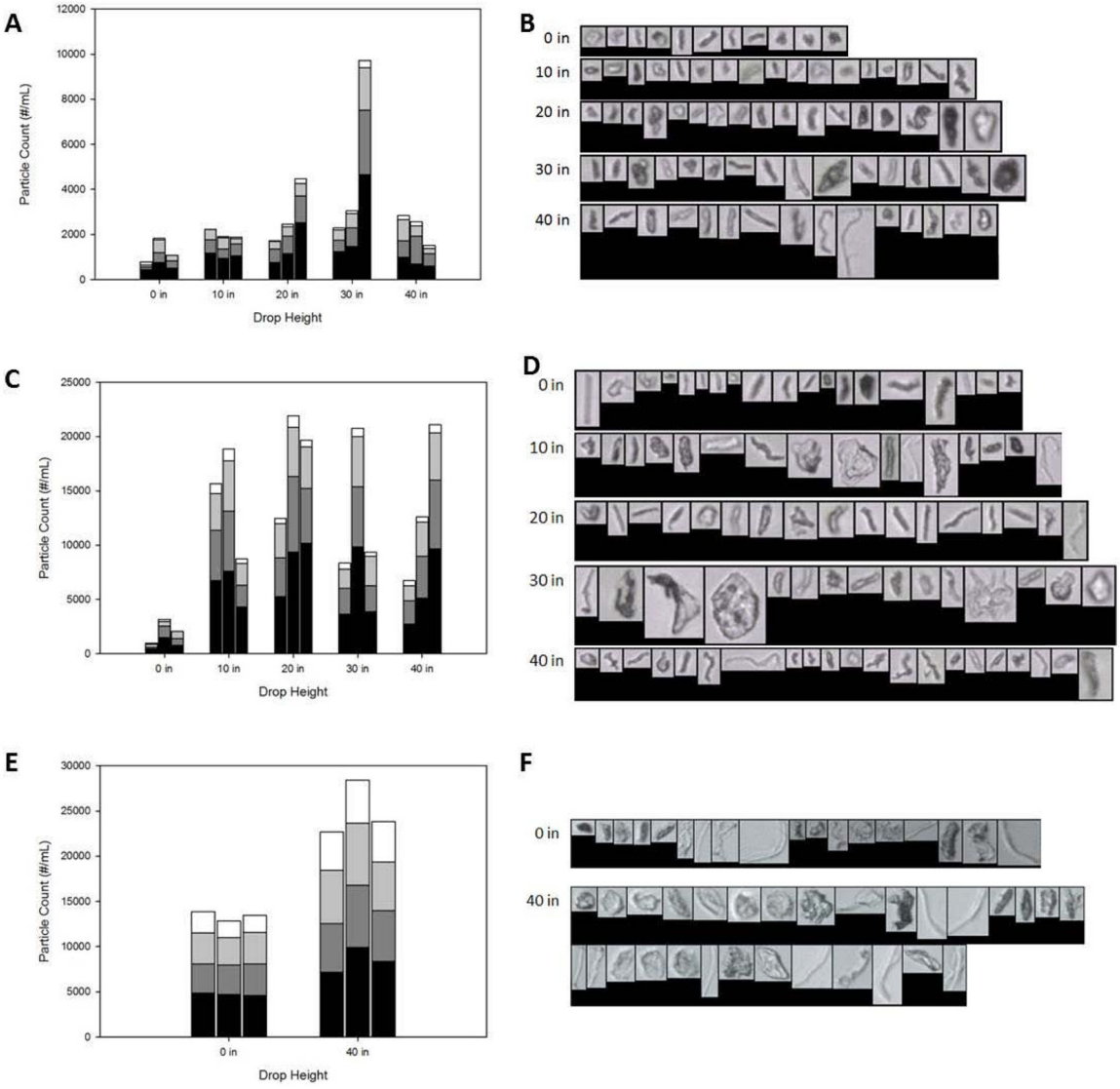

Figure 8.

Particle counts and examples of particle morphologies for shock treated 1 mg/mL antistreptavidin (A,B), 35 mg/mL antistreptavidin (C,D), and 1.75 mg/mL human growth hormone (E,F). The black portion of each bar represents particles with diameters at least 2 microns and less than 3 microns, the dark grey portion represents particles with diameters at least 3 microns and less than 5 microns, the light grey portion represents particles with diameters at least 5 microns and less than 10 microns, and the white portion represent particles with diameters at least 10 microns. Each bar represents the particle count from one vial.

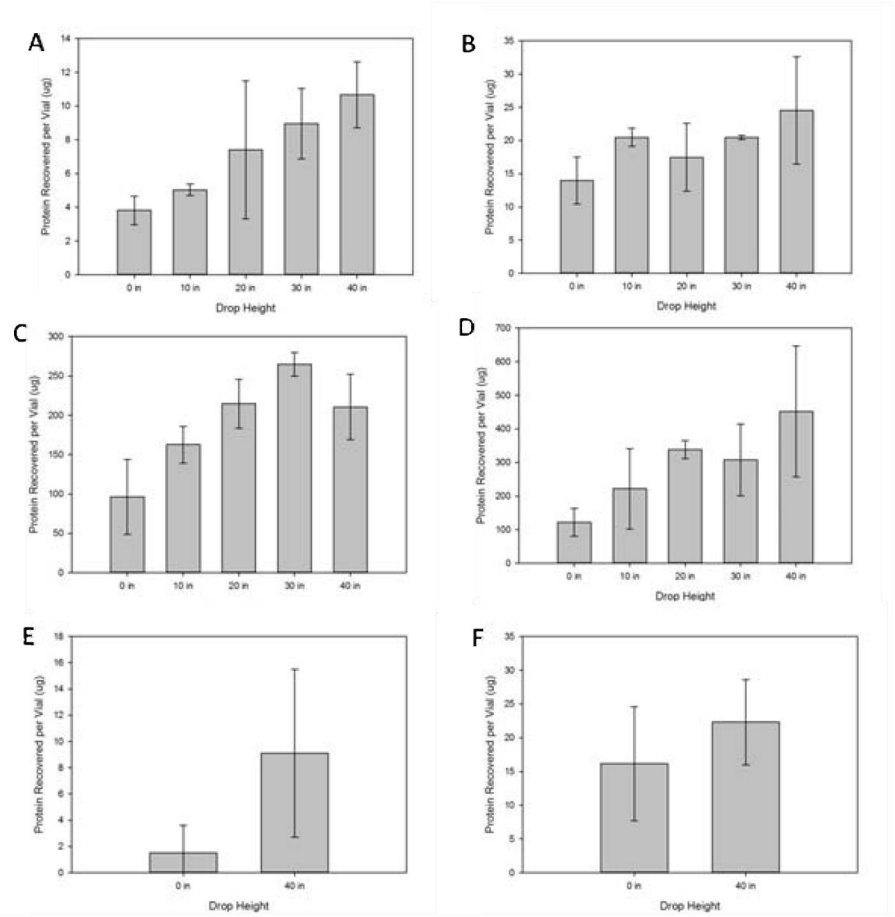

Figure 9.

Amount of protein recovered from the walls of dropped vials following treatment with urea (A,C,E) or guanidine hydrochloride (B,D,F). Dropped vials contained 1 mg/mL antistreptavidin (A,B), 35 mg/mL antistreptavidin (C,D), or 1.75 mg/mL human growth hormone (E,F)